ALADIN-Based Coordinated Operation of Power Distribution and Traffic Networks with Electric Vehicles

Guangzeng Sun, *Student Member, IEEE,* Gengyin Li, *Member, IEEE,* Shiwei Xia, *Senior Member, IEEE,* Mohammad Shahidehpour, *Fellow, IEEE,* Xi Lu, Ka Wing Chan, *Member, IEEE*

[1] ***Abstract***—Electric vehicles (EVs) are recognized as a promising remedy for the environmental crisis and fuel shortage faced by modern metropolises. But meanwhile, with the popularization of EVs, the unordered charging of EVs will have negative impacts on both the power distribution network (DN) and the traffic network (TN). The well scheduled EV charging/discharging behaviors could participate in the coordinated operation of TN and DN to significantly enhance the energy utilization efficiency of both networks. With an assumption that an entity like State Grid capable of dispatching distributed generators (DGs) and adjusting charging prices of fast charging stations (FCSs), a traffic-distribution coordination (TDC) model is proposed to minimize the travel cost of TN and energy service cost of DN, which simultaneously considers the economic operation of DN by alternating current dynamic optimal power flow (AC DOPF) and the traffic flow assignment of TN by EVs dynamic user equilibrium (DUE) respectively. And afterward the augmented Lagrangian alternating direction inexact Newton (ALADIN) method is adopted to solve the TDC model. Finally, the necessity of coordinated operation of TN and DN and the effectiveness of TDC model are validated in an integrated system of modified Nguyen-Dupius TN and IEEE 33-bus DN.

Index Terms—traffic-distribution coordination with electric vehicles, alternating current dynamic optimal power flow, dynamic user equilibrium, augmented Lagrangian alternating direction inexact Newton.

I. Introduction

With growing concern about carbon emission, pollution and oil depletion issues, the trend in replacing fossil-fueled cars with electric vehicles (EVs) is inevitable. The total number of electric vehicles on the road has reached 5.1 million in 2019 and will increase to more than 100 million by 2030 [1]-[2]. The proliferation of EVs will have remarkable impacts on operations of distribution network (DN) and traffic network (TN). Fast charging stations (FCSs) on road would simultaneously have an impact traffic flow in TN and power flow in DN, thereby couple the two networks tightly. However, EV dispatch scheduling in separate TN or DN has been the subject of study for many years; but the corresponding results have often pointed to sub-optimal solutions. The interdisciplinary research on the coordinated operation of TN and DN has significantly enhanced the operation efficiency and ensure the safe operation of DN. The coordination of the two networks labeled as the traffic-distribution coordination (TDC) model can be used in the future as a fundamental analytical tool for infrastructure planning, EV scheduling, and economic operation of electrified transportation network.

In the realm of DN, EVs are characterized as mobile and distributed energy storage devices, which can participate in demand response programs [3]. Vehicle-to-grid enables EVs to either inject power to or draw power from the grid for peak shaving and valley filling [4]. Besides, EVs can provide auxiliary services and enhance the operational flexibility of power systems in particular as resource variability in power systems is heightened [5]-[6]. The impact of EV charging facilities on DN operation was assessed in [7]-[8]. When EVs play a significant role in DN operations, the intertemporal feature of EVs charging transforms the traditional optimal power flow problem into a dynamic optimal power flow problem [9].

As for TN operation, the research has mainly focused on EVs' route charging navigation. In [10], a route optimization model of the alternative energy-fueled vehicles was presented, which minimized the travelling distance with consideration of the alternative energy supply and the maximum fuel capacity limit. Compared with [10], the charging cost and battery capacity of EVs were considered in the route selection model with the assumption that the charging price is constant [11]. To relax this assumption, a time-of-use electricity price based route optimization model was further developed in [12] to reflect the interaction of route selection and electricity price. Different from these deterministic route selection model used in [10]-[12], the charging navigation model both in deterministic and stochastic traffic network was proposed in [13] to improve the navigation accuracy.

With regard to the TN and DN coordinated operation, the traffic flow of TN and power flow of DN should be considered simultaneously. The user equilibrium (UE) model considering the range anxiety of EVs was proposed in [14], and was further improved to include trip chains in [15]. However, the capacities of FCSs were neglected. In [16], a battery capacity-constrained flow-capturing location model was presented to maximize EV traffic flow in charging stations. In [17], a decentralized optimization framework was proposed to analyze the impact of wireless charging on TN and DN, and the UE traffic assignment and the day-ahead electricity market operation were simultaneously considered. Similar to [17], an equilibrium

This work was supported partially by The Smart Grid Joint Foundation Program of National Natural Science Foundation of China and State Grid Corporation of China (U1966204), the Jiangsu Basic Research Project (Natural Science Foundation BK20180284), the Fundamental Research Funds for the Central Universities (2019MS007), and the China National Study Foundation (201906735013).

G. Sun, G. Li and S. Xia are with the State Key Laboratory of Alternate Electrical Power System with Renewable Energy Sources, North China Electric Power University, Beijing 102206, China (e-mail: sunguangzeng@yeah.net; ligy@ncepu.edu.cn; s.w.xia@ncepu.edu.cn).

M. Shahidehpour is with Illinois Institute of Technology, Chicago, IL 60616 USA. He is also a Research Professor with the Center of Research Excellence in Renewable Energy and Power Systems, King Abdulaziz University, Jeddah, Saudi Arabia (e-mail: ms@iit.edu).

X. Lu and K. W. Chan are with the Department of Electrical Engineering, The Hong Kong Polytechnic University, Hung Hom, Hong Kong. (e-mail: harry.lu@connect.polyu.hk; eekwchan@polyu.edu.hk).

model integrating the stochastic UE and direct current optimal power flow was developed to study the interaction between traffic flow and electricity prices [18]-[19]. In [20]-[22], a hybrid model consisting of the traffic assignment of TN and optimal power flow of DN was designed to minimize the social cost by optimally schedule the generation of DGs and charge the congestion tolls on congested roads. Different from the UE based model in [14]-[22], [23] proposed a socially optimum (SO) model to enable the TN and DN operators to cooperatively manage the TN and DN network towards a SO operating point. All these studies adopt the static UE or SO method to assign traffic flows, however the time-varying traffic demands and intertemporal EVs charging behaviors are not considered.

In this paper, the TDC model is proposed to minimize the travel cost of TN and energy service cost of DN by simultaneously considering the dynamic user equilibrium (DUE) of TN and the alternating current dynamic optimal power flow (AC DOPF) of DN. However, the TDC model is difficult to solve because it engages a large number of control variables and constraints. Correspondingly, a distributed algorithm based on augmented Lagrangian alternating direction inexact Newton (ALADIN) is adopted to solve the TDC model in this paper.

Similar to alternating direction of multipliers method, ALADIN solves a sequence of local optimization problems combined with a coordination step. The complicated operations are performed locally in which the iterative TDC solution is based on a quadratic objective function with linear equality constraints [24]. However, in contrast to the alternating direction of multipliers method, the sequential quadratic programming is applied to improve the updating step of ALADIN with a faster convergence rate, which requires fewer ALADIN iterations than that of alternating direction of multipliers method by an order of magnitude.

The main contributions of this paper are threefold as follows:

1) DUE is first established to consider time-varying traffic demands and intertemporal EV charging behaviour, which are ignored or simplified in previous studies [14]-[23]. In addition, transfer and dummy arcs are designed to represent FCSs as a transit TN module, and the capacities of FCSs are also considered in the performance function of transfer arc, which have been neglected in [14]–[15], [18]–[19] and [22].

2) The TDC model is proposed to minimize the travel cost of TN and energy service cost of DN, which simultaneously takes into account the DN dynamic economic operation and TN dynamic traffic assignment. In the model, AC DOPF of DN is presented to optimize the locational marginal prices during multiple time periods for coordinating TN and DN operation, meanwhile the nodal voltage restrictions, DGs' ramp up/down constraints and network losses are fully considered, which have been ignored in [17]-[18] and [23]. Moreover, the ALADIN distributed algorithm is applied to efficiently solve the proposed TDC model with a large number of coupling variables and constraints.

3) An integrated system of modified Nguyen-Dupius TN and IEEE 33-bus DN is tested to validate the effectiveness of the proposed TDC model. Simulation results demonstrate that the optimal traffic and power flows are effectively obtained through the TDC model, and potential risks of DN voltage violations are well mitigated by adjusting FCS charging prices in TN.

The rest of this paper is organized as following. The TDC model simultaneously considering DUE of TN and AC DOPF of DN is proposed in Section II, and then a distributed algorithm ALADIN is presented in Section III to solve the TDC model. In Sections IV, a case study consisting of TN and DN is designed to validate the effectiveness of TDC model with conclusions given in the last section.

II. TDC Model Formulation

The TDC model is proposed in this section to minimize the sum of travel cost of TN and energy service cost of DN, which simultaneously considers DUE in TN and AC DOPF in DN as follows.

A. DUE in TN

1) Definition and Assumptions

UE is an effective measure to assign traffic flows to an urban TN. However, the traditional UE is not suitable for considering time-varying traffic demands and intertemporal EV charging features. Therefore, we use DUE in this paper to solve the traffic assignment problem with time-varying traffic demands and intertemporal EVs charging behaviors. Before establishing the mathematical model, the DUE definition and corresponding assumptions are put forward as follows.

DUE Definition: For any EV leaving its origin at any time for destination, the EV travel costs on any used paths are equal and minimal; and the EV travel costs on any unused paths are larger than or equal to those on used paths [25].

Assumptions:

i) The path selection rule for every EV is to minimize the travel cost from origin to destination based on the assumption that travellers can obtain the complete information on TN traffic arcs and FCS charging prices before selecting any paths. This is a traditional assumption in the research of transportation field [26], and with the development of 5G communication technology and intelligent transportation system, it is reasonable to know the traffic flow on arcs of every feasible path and charging prices of FCSs before choosing travel path.

ii) The charging ratio of each O-D pair is γ and the average EV charging energy is used in place of individual EV charging to simplify the TDC model. That means EV assigned to an FCS receives the average energy E_{ch} with an average charging power P_{ch} [27]. We will accordingly refine the proposed solution by aggregating all EVs into several categories for representing different charging energy and power. Since this paper focuses on the coordinated operation of TN and DN in a system-level, it is acceptable to utilize the average EV charging energy instead of the heterogeneous EV information for establishing TDC.

2) Network Representation

The TN is represented by a connected graph $G_{TN} = (V, A)$, where V denotes the set of consecutively numbered vertices, which include TN origins, destinations and intersections; A denotes the set of consecutively numbered arcs (links), representing lanes or roadway segments. The TN topology is depicted by a vertex-arc incidence matrix $M^{|V|\times|A|}$ with elements $\mu_{v,a}$, where $\mu_{v,a}$=1(-1) represents the vertex v is the entrance (exit) associated with the arc a. Let $A_{en}(v)$ denote the set of arcs with an entrance vertex v where $A_{ex}(v)$ denotes the set of arcs with an exit vertex v. Let R denote the set of origins (which initiate traffic flows) and S denote the set of destinations (which

terminate traffic flows). Note that $R \cap S \neq \varnothing$ since TN vertices can serve as origins and destinations for different simultaneous trips. Each O-D pair *r*-*s* is connected by a set of paths (routes) through TN. This path set is denoted by K_{rs} where $r \in R$ and $s \in S$. Let Δ_{rs} denote the arc-path incidence matrix for O-D pair *r*-*s* with element $\delta_{a,k}^{rs}$, where $\delta_{a,k}^{rs}=1$ if arc *a* is a part of path *k* (where $k \in K_{rs}$) connecting O-D pair *r*-*s*; otherwise $\delta_{a,k}^{rs}=0$.

The origin-destination matrix is denoted by $Q(t)$ with entries $q_{rs}(t)$ representing the traffic demand between origin *r* and destination *s* during the time slot *t*. Let $x_a(t)$ represent the traffic flow assigned to arc *a* at time slot *t*. Let $f_k^{rs}(t)$ denote the traffic flow assigned to path *k* connecting origin *r* and destination *s* at time slot *t*. Let $O_a^s(t)$ denote the traffic outflow with destination *s* on arc *a* at time slot *t*. The traffic outflow on arc *a* at time slot *t* is denoted by $O_a(t)$, where $O_a(t)=\sum_s O_a^s(t)$. The traffic flow on arc *a* at time slot *t* is denoted by $e_a(t)$.

FCSs is a linking infrastructure for connecting TN and DN. In [28], an FCS was considered a charging route destination in TN, which was not distinguished from ordinary vertices. However, an FCS is often located along the path rather than TN origins, destinations and intersections. In this paper, transfer and dummy arcs are introduced in the TDC model, and FCS is represented by a transit module in Fig. 1. The transit module consists of two vertices, which include a transfer arc for EV charging and a dummy arc with zero travel time. Under this characterization, TN arcs are classified into three types of ordinary (A_O), transfer (A_T)and dummy (A_D) arcs with different performance functions, where $A_O \cup A_T \cup A_D = A$.

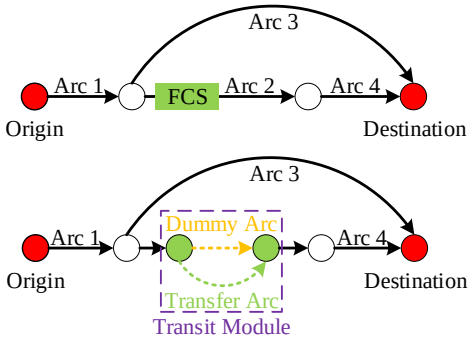

Fig. 1. A TN graph with FCS

In urban TN, the travel time on urban streets and intersections increases with traffic flow because of traffic congestion. Consequently, the arc performance function $t_a(e_a(t))$ relates the arc travel time and flow $e_a(t)$. The performance functions of ordinary, transfer, and dummy arcs are presented as follows.

i) Ordinary arcs without FCS. A practical function is developed by the U.S. Bureau of Public Roads (BPR) [29] as

$$t_a(e_a(t)) = t_a^0\left[1+0.15\left(\frac{e_a(t)}{c_a}\right)^4\right], a \in A_O \quad (1)$$

where t_a^0 is the free-flow travel time, i.e., the length of link divided by the speed limit, and c_a is the capacity of arc *a*. Also, e_a/c_a is the saturation widely used in traffic engineering. Equation (1) is the performance function of ordinary arcs, which represents the travel time of arc *a* ($a \in A_O$) at time *t*.

ii) Transfer arcs for charging. The travel time on this arc consists of charging and queueing times. The Davidson function developed in [30] by using the the queuing theory is introduced and modified for representing the arc performance.

$$t_a(e_a(t)) = t_a^{ch}\left\lceil \frac{e_a(t)}{c_a^{ch}} \right\rceil \left[1+J\left(\frac{e_a(t)-c_a^{ch}\left\lfloor \frac{e_a(t)}{c_a^{ch}} \right\rfloor}{c_a^{ch}-\left[e_a(t)-c_a^{ch}\left\lfloor \frac{e_a(t)}{c_a^{ch}} \right\rfloor\right]}\right)\right], a \in A_T \quad (2)$$

where t_a^{ch} is the charging time according to assumption ii which is stated as $t_a^{ch}=E_{ch}/P_{ch}, \forall a \in A_T$). c_a^{ch} is the FCS capacity of on the transfer arc *a*. $\lfloor \bullet \rfloor$ ($\lceil \bullet \rceil$) represents round down (up) to an integer. *J* is the curvature parameter which controls the shape of the curve. Equation (2) is the performance function of transfer arcs, which represents the travel time of arc a ($a \in A_T$) at time *t* including charging time and queueing time.

iii) Dummy arcs. The dummy arc is introduced to ensure the connectivity of TN. Since the length of dummy arc is very short, the travel time on this arc is negligible and the dummy arc performance function is given by

$$t_a(e_a(t)) = 0, a \in A_D \quad (3)$$

For each O-D pair, EV can travel *r* to *s* through a chain of connected arcs, which is referred to a feasible path. The feasible path only depends on the TN topology and EV charging demand. We assume the charging ratio of each O-D pair is γ, which means γ percent EVs of the total traffic demand need to be charged for arriving at the destination. In other words, a feasible EV path must include transfer arcs for an O-D pair extending from *r* to *s*. The set of feasible paths which includes transfer arcs is represented by K_{rs}^T; the set of feasible paths without transfer arcs is denoted by K_{rs}^O.

3) DUE of Traffic Network

The DUE objective is to minimize the total travel cost C_{TN}.

$$\min \quad C_{TN} = \sum_{t \in T}\left[\begin{array}{l}\sum_{a \in A_O}\int_{e_a(t-1)}^{e_a(t)} \beta t_a(\theta)d\theta \\ +\sum_{a \in A_T}\left(\int_{e_a(t-1)}^{e_a(t)} \beta t_a(\theta)d\theta + \lambda_a^j E_{ch} e_a(t)\right)\end{array}\right] \quad (4)$$

The first term in (4) is the travel time cost in ordinary arcs, the second term is the sum of time and charging costs of transfer arcs, where β is the monetary price of time, and λ_a^j denotes both the FCS charging price on transfer arc $a \in A_T$ and locational marginal prices of bus *j* in DN.

Based on the traditional dynamic traffic assignment model [31], considering operation characteristic of FCSs and EVs, the DUE constraints are developed as follows.

$$\sum_{k \in K_{rs}^T} f_k^{rs}(t) = \gamma q_{rs}(t) + \sum_{a \in A_{ex}(r) \cap A_T} O_a^s(t) \quad (5)$$

$$\sum_{k \in K_{rs}^O} f_k^{rs}(t) = (1-\gamma) q_{rs}(t) + \sum_{a \in A_{ex}(r) \cap (A_O \cup A_D)} O_a^s(t) \quad (6)$$

$$x_a(t) = \sum_{r \in R}\sum_{s \in S}\sum_{k \in K_{rs}} f_k^{rs}(t)\delta_{a,k}^{rs} \quad (7)$$

$$e_a(t) = e_a(t-1) + x_a(t) - O_a(t) \quad (8)$$

$$O_a(t) = \sum_{s \in S} O_a^s(t) \quad (9)$$

$$f_k^{rs}(t) \geq 0 \quad (10)$$

$$\lambda_a^j \geq \lambda_{\min} \quad (11)$$

$$e_a(0) = 0 \quad (12)$$

In this model, (5) and (6) represent traffic flow conservation constraints. Accordingly, for each O-D pair *r*-*s*, traffic flows assigned to all feasible paths at *r* are equal to the sum of traffic demands originated at other vertices, which stops in *r* before

arriving at *s*. Equation (7) defines the relationship between arc flow and path flow. Equation (8) and (9) represent the traffic flow coupling between *t* and *t*-1. For each arc, the traffic flow difference between time slots *t* and *t*-1 is equal to the difference between the traffic flow assigned to time slot *t* and the traffic outflow at time slot *t*. The non-negative conditions of (10) are designed to ensure that the solution will be physically attainable. Equation (11) ensures that C_{TN} will be reduced by adjusting traffic flow assignments rather than cutting the FCSs charging prices. Equation (12) indicates that the initial traffic flow on each arc is zero.

To proof the optimal solution of mathematical model (4)-(12) satisfying the DUE definition as presented above, the objective function $C_{TN}(e_a(t))$ can be transferred to $C_{TN}(f_k^{rs}(t))$ using (7) and (8). The corresponding Lagrangian function is formulated as:

$$L(f_k^{rs}(t),\rho_{rs}^t)=C_{TN}(f_k^{rs}(t))+\sum_{rs}\rho_{rs}^t\left(q_{rs}(t)+\sum_{a\in A_{ex}(r)}O_a^s(t)-\sum_k f_k^{rs}(t)\right) \quad (13)$$

The first-order conditions of the mathematical model consisting of (4)-(12) are equivalent to the first-order condition of Lagrangian function (13), given that (13) has to be minimized with respect to (10). The first-order condition of (13) is given as follows.

$$\begin{cases} f_k^{rs}(t)\dfrac{\partial L(f_k^{rs}(t),\rho_{rs}^t)}{\partial f_k^{rs}(t)}=0,\forall k,r,s \\ \dfrac{\partial L(f_k^{rs}(t),\rho_{rs}^t)}{\partial f_k^{rs}(t)}\ge 0,\forall k,r,s \\ \dfrac{\partial L(f_k^{rs}(t),\rho_{rs}^t)}{\partial \rho_{rs}^t}=0,\forall r,s \\ f_k^{rs}(t)\ge 0,\forall k,r,s \end{cases} \quad (14)$$

If we substitute (4) into (13), the partial derivative of Lagrangian function is given as:

$$\begin{aligned} &\frac{\partial}{\partial f_l^{mn}(t)}L(f_k^{rs}(t),\rho_{rs}^t) \\ &=\frac{\partial}{\partial f_l^{mn}(t)}\left[C_{TN}(f_k^{rs}(t))+\sum_{rs}\rho_{rs}^t\left(\begin{matrix}q_{rs}(t)\\+\sum_{a\in A_{ex}(r)}O_a^s(t)-\sum_k f_k^{rs}(t)\end{matrix}\right)\right] \\ &=\frac{\partial C_{TN}(e_b(t))}{\partial e_b(t)}\frac{\partial e_b(t)}{\partial x_b(t)}\frac{\partial x_b(t)}{\partial f_l^{mn}(t)}+\frac{\partial}{\partial f_l^{mn}(t)}\sum_{rs}\rho_{rs}^t\left(-\sum_k f_k^{rs}(t)\right) \\ &=\left(\sum_{b\in A_O}\beta t_b(e_b(t))+\sum_{b\in A_T}(\beta t_b(e_b(t))+\lambda_b^j E_{ch})\right)\delta_{b,l}^{mn}-\rho_{mn}^t \end{aligned} \quad (15)$$

Let $c_l^{mn}(t)=\left(\sum_{b\in A_O}\beta t_b(e_b(t))+\sum_{b\in A_T}(\beta t_b(e_b(t))+\lambda_b^j E_{ch})\right)\delta_{b,l}^{mn}$ denote the travel cost on path *l* which is extended from *m* to *n*. The first-order condition (14) can be transfered to (16) using (15).

$$\begin{cases} f_k^{rs}(t)\left(c_k^{rs}(t)-\rho_{rs}^t\right)=0,\forall k,r,s \\ c_k^{rs}(t)-\rho_{rs}^t\ge 0,\forall k,r,s \\ \sum_k f_k^{rs}(t)=q_{rs}(t)+\sum_{a\in A_{ex}(r)}O_a^s(t),\forall r,s \\ f_k^{rs}(t)\ge 0,\forall k,r,s \end{cases} \quad (16)$$

Here, (16) indicates that if path *k* connecting *r*-*s* is in use (i.e. $f_k^{rs}(t)>0$), the travel cost on this path is $c_k^{rs}(t)=\rho_{rs}^t$; if the travel cost $c_k^{rs}(t)>\rho_{rs}^t$, the path *k* is unused (i.e. $f_k^{rs}(t)=0$). Thus ρ_{rs}^t is equal to the minimum path travel cost between *r* and *s*. The above analyses and derivations, point out that the optimal solution of the mathematical model (4)-(12) satisfies the DUE definition.

B. AC DOPF of DN

DN is composed of buses and lines commonly located in a radial manner. Without the loss of generality, a radial DN is considered in this paper which is represented by a directed graph $G_{DN}=(N, L)$. Let $N=\{1,\ldots,N\}$ denote the set of all buses, bus 1 as the substation bus, the other buses as $N^+=\{2,\ldots,N\}$. Each pair (i,j) in *L* represents a line with impedance $z_{ij}=r_{ij}+ix_{ij}$, and P_{ij}^t and Q_{ij}^t denote active and reactive power from bus *i* to *j*, respectively. Let $\Omega(i)$ denote the collections of buses stemming from bus *i*. A typical tree graph of radial distribution network is shown in Fig. 2. Let $T=\{1,\ldots,T\}$ denote the set of time slots. For each bus $j\in\Omega(i)$, $k\in\Omega(j)$, at time $t\in T$, the AC DOPF of DN is given as follows [32]-[33].

$$P_{DG,j}^t+P_{ij}^t-r_{ij}\ell_{ij}^t=\sum_{k\in\Omega(j)}P_{jk}^t+P_{load,j}^t+P_{FCS,j}^t,\ j\in N^+ \quad (17)$$

$$Q_{DG,j}^t+Q_{ij}^t-x_{ij}\ell_{ij}^t=\sum_{k\in\Omega(j)}Q_{jk}^t+Q_{load,j}^t,\ j\in N^+ \quad (18)$$

$$\upsilon_i^t-\upsilon_j^t=2(r_{ij}P_{ij}^t+x_{ij}Q_{ij}^t)-(r_{ij}^2+x_{ij}^2)\ell_{ij}^t,\ j\in N^+ \quad (19)$$

$$\upsilon_i^t\ell_{ij}^t=(P_{ij}^t)^2+(Q_{ij}^t)^2,\ j\in N^+ \quad (20)$$

$$P_{DG,j}^{\min}\le P_{DG,j}^t\le P_{DG,j}^{\max},\ j\in N^+ \quad (21)$$

$$Q_{DG,j}^{\min}\le Q_{DG,j}^t\le Q_{DG,j}^{\max},\ j\in N^+ \quad (22)$$

$$\upsilon_j^{\min}\le\upsilon_j^t\le\upsilon_j^{\max},\ j\in N \quad (23)$$

$$-r_d\Delta t\le P_{DG,j}^t-P_{DG,j}^{t-1}\le r_u\Delta t,\ j\in N^+ \quad (24)$$

In this model, (17)-(20) represent branch flows, where $P_{DG,j}^t$ and $Q_{DG,j}^t$ are active and reactive power of DGs at bus *j* at time slot *t*. $P_{load,j}^t$ and $Q_{load,j}^t$ are active and reactive demand at bus *j*. υ_j^t denotes the square of voltage magnitude at bus *j*, and ℓ_{ij}^t denotes the square of current magnitude of line (i,j). $P_{FCS,j}^t$ denotes the total charging power of FCS at bus *j*, which is given by

$$\boldsymbol{P}_{FCS,j}^t=\varepsilon_a^j e_a(t)P_{ch},\boldsymbol{a}\in\boldsymbol{A}_T \quad (25)$$

where ε_a^j is the element of traffic-power incidence matrix, where $\varepsilon_a^j=1$ if the corresponding FCS on arc *a* of TN is connected to bus *j* of DN; otherwise, $\varepsilon_a^j=0$. $e_a(t)$ is the traffic flow on arc $a\in A_T$ in TN, and P_{ch} is the EV charging power in FCS.

Equations (21)-(23) represent the active and reactive power bounds of DGs, as well as square voltage magnitude bounds at bus *j*. Equation (24) represents the ramp up and down constraints of DGs with the upper limits r_u and lower limits r_d. Equation (25) represents charging demand of FCS.

The objective of AC DOPF can be expressed as (26).

$$\min\quad C_{DN}=\sum_{t\in T}\left[\sum_{j\in N}\left[a_j(P_{DG,j}^t)^2+b_jP_{DG,j}^t\right]+\lambda_b\sum_{j\in\Omega(1)}P_{1j}^t\right] \quad (26)$$

The energy service cost C_{DN} consists of two terms. The first term is the production cost of DGs in DN. P_{1j}^t denotes the active power directly delivered from the substation bus 1, and λ_b is the price of purchasing electricity from the main grid; hence the second term is the purchase payment.

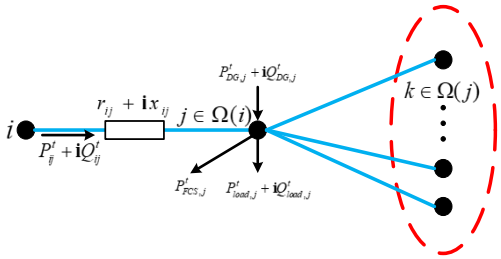

Fig. 2. Tree graph of a radial distribution network

C. TDC Model

The traffic information of arcs, congestion condition and FCS charging prices in TN will influence the EV traffic flow assignment. The EV spatial and temporal distribution will impact the electricity load profile and DN operations. The coordinated operation of TN and DN can be implemented by an entity like the State Grid with capability of dispatching DGs and adjusting FCSs charging prices. The proposed TDC model will minimize the sum of travel cost of TN and energy service cost of DN, which simultaneously considers the DN economic operations and EV traffic flow assignments in TN. The proposed TDC model is stated as follows.

$$\min \quad C_{TDC} = \sum_{t\in T} C_{TN}(t) + C_{DN}(t) \tag{27}$$

subject to:

Constraints of TN (5)-(12)
Constraints of DN (17)-(25)

From TN side, charging prices λ_a^j are included in both the objective function (4) and constraint (11), and the traffic flow of all arcs is optimized with an initial charging price and afterward passed to DN. From DN side, the charging demand of FCS is calculated by (25) based on the optimized traffic flow in TN, and then the locational marginal prices are determined from AC DOPF of DN and passed to TN. This procedure is iteratively repeated for representing the interactions of TN and DN, and the proposed TDC model will be finally solved when the charging prices and locational marginal prices reach equilibrium.

III. TDC SOLUTION ALGORITHM

In this section, we discuss the TDC convex transformation and present the distributed ALADIN algorithm to solve the TDC model.

A. Convex Transformation of TDC model

The convexity of DUE analyses and the second-order cone programming relaxation of AC DOPF are prepared here for the convex transformation of TDC model.

1) Convexity of DUE

The DUE constraints are affine and DUE is a convex optimization problem if the Hessian matrix of (4) is positive definite.

$$\begin{aligned}\frac{\partial C_{TN}}{\partial x_m(t)} &= \frac{\partial}{\partial x_m(t)}\sum_{t\in T}\left[\sum_{a\in A_O}\int_{e_a(t-1)}^{e_a(t)}\beta t_a(\theta)d\theta + \sum_{a\in A_T}\left(\int_{e_a(t-1)}^{e_a(t)}\beta t_a(\theta)d\theta + \lambda_a^j E_{ch} e_a(t)\right)\right]\\ &= \frac{\partial}{\partial e_m(t)}\sum_{t\in T}\left[\begin{array}{l}\sum_{a\in A_O}\int_{e_a(t-1)}^{e_a(t)}\beta t_a(\theta)d\theta \\ +\sum_{a\in A_T}\left(\int_{e_a(t-1)}^{e_a(t)}\beta t_a(\theta)d\theta + \lambda_a^j E_{ch} e_a(t)\right)\end{array}\right]\frac{\partial e_m(t)}{\partial x_m(t)}\\ &= t_m(e_m(t))\big|_{m\in A_O} + \left[t_m(e_m(t)) + \lambda_m^j E_{ch}\right]\big|_{m\in A_T}\end{aligned} \tag{28}$$

$$\begin{aligned}\frac{\partial C_{TN}}{\partial x_m(t)\partial x_n(t)} &= \frac{\partial}{\partial x_n(t)}\left[t_m(e_m(t))\big|_{m\in A_O} + \left[t_m(e_m(t)) + \lambda_m^j E_{ch}\right]\big|_{m\in A_T}\right]\\ &= \begin{cases}\left.\dfrac{dt_n(e_n(t))}{de_n(t)}\right|_{m\in A_O} + \left.\dfrac{dt_n(e_n(t))}{de_n(t)}\right|_{m\in A_T} & m = n\\ 0 & m \neq n\end{cases}\end{aligned} \tag{29}$$

Equations (28) and (29) are the first-order and second-order partial derivatives of (4), respectively. In (28) and (29), all off-diagonal elements of Hessian $\nabla^2 C_{TN}$ are zero and all diagonal elements are given by $dt_a(e_a(t))/de_a(t)$, where $a\in A_O$ or $a\in A_T$. Hence

$$\nabla^2 C_{TN} = diag\left[\frac{dt_1(e_1(t))}{de_1(t)},\ldots,\frac{dt_{|A|}(e_{|A|}(t))}{de_{|A|}(t)}\right] \tag{30}$$

The Hessian matrix (30) is a diagonal positive definite matrix with all entries strictly positive, $dt_a(e_a(t))/de_a(t)>0$, because of monotone increase in arc performance functions (1) and (2). Therefore, the objective function (4) is strictly convex and DUE is a convex optimization problem.

2) second-order cone programming relaxation of AC DOPF

The AC DOPF constraints satisfy the convex optimization requirements, except for (20). In [34]-[35], the non-convex equality constraint (20) is relaxed to inequality constraints by the second-order cone programming relaxation method as follows:

$$\upsilon_i^t \ell_{ij}^t \geq (P_{ij}^t)^2 + (Q_{ij}^t)^2,\ j \in N^+ \tag{31}$$

Accordingly, the proposed TDC model is formulated as a convex optimization problem.

$$\begin{aligned}\min \quad & C_{TDC} = \sum_{t\in T} C_{TN}(t) + C_{DN}(t)\\ s.t. \quad & Constraints\ of\ TN\ (5)-(12)\\ & Constraints\ of\ DN\ (17)-(19),\ (21)-(25),\ (31)\end{aligned} \tag{32}$$

B. ALADIN-based TDC model

On one hand, it is not easy to directly solve the TDC model due to a large number of optimization variables and the hybrid objective; on the other hand, the variables and integrated objective of original TDC model can be separated into the TN and DN sub-problems with coupled affine constraints, and thereby TDC model would be effectively solved by a divide and conquer strategy. While ALADIN is such a kind of algorithm, which are well designed for solving sub-problems with separable objective and coupled affine constraints based on augmented Lagrangian theory [36], therefore the ALADIN algorithm is presented in this paper to optimize the proposed TDC model as follows.

$$\begin{aligned}\min_z \quad & \sum_{i=1}^{N} f_i(z_i)\\ s.t. \quad & \begin{cases}\sum_{i=1}^{N} A_i z_i = 0\\ h_i(z_i) \leq 0, i \in \{TN, DN\}\end{cases}\end{aligned} \tag{33}$$

Summarizing the above, the TDC model (32) can be reformulated in a affinely coupled separable form as (33). Here, the TN variables are integrated as $z_{TN}^t=[f_k^{rs}(t)]^{\mathrm{Tr}}$ for every path $k\in K_{rs}, \forall r,s$, and DN variables are integrated as $z_{DN}^t=[\upsilon_j^t, \ell_{ij}^t, (P_{jk}^t)^{\mathrm{Tr}}, (Q_{jk}^t)^{\mathrm{Tr}}]^{\mathrm{Tr}}$ for bus $j\in N$, where $[\bullet]^{\mathrm{Tr}}$

represents the transpose of a matrix. Let $z_{TN}=[z_{TN}^1,\ldots,z_{TN}^T]^{\mathrm{Tr}}$ and $z_{DN}=[z_{DN}^1,\ldots,z_{DN}^T]^{\mathrm{Tr}}$; accordingly, the TDC objective function is represented as.

$$\min \quad f_{TN}(z_{TN})+f_{DN}(z_{DN}) \tag{34}$$

The TN equations (5)-(12) are formulated as nonlinear equality constraints $h_{TN}(z_{TN})\le 0$, and (17)-(19), (21)-(24), (31) of DN are formulated as nonlinear equality constraints $h_{DN}(z_{DN})\le 0$. Here, (25) are formulated as affine consensus constraints $A_{TN}z_{TN}+A_{DN}z_{DN}=0$. Applying the ALADIN theory [36], we present the technical details of ALADIN in Algorithm 1 to solve the proposed TDC model.

Algorithm 1: ALADIN to solve TDC model

1) **Initialization**: Initial guess (s_0,λ_0); penalty parameters ρ, $\mu=\underline{\mu}$; weighting matrix $\sum_i$, and tolerance ε

2) **While** $\|A_{TN}z_{TN}+A_{DN}z_{DN}\|_\infty>\varepsilon$ and $\left\|\begin{pmatrix}z_{TN}\\z_{DN}\end{pmatrix}-\begin{pmatrix}s_{TN}\\s_{DN}\end{pmatrix}\right\|_\infty>\varepsilon$ **do**

3) Solve the decoupled NLPs for all $z_i\in\{z_{TN},z_{DN}\}$

$$\min_{z_i} \quad f_i(z_i)+\lambda A_i z_i+\frac{\rho}{2}\|z_i-s_i\|_{\sum_i}^2$$
$$s.t. \quad h_i(z_i)\le 0 \,|\kappa_i$$

4) Compute Jacobians, gradients and Hessians for all $z_i\in\{z_{TN},z_{DN}\}$, $s_i\in\{s_{TN},s_{DN}\}$

$$C_{i,j}=\begin{cases}\dfrac{\partial}{\partial s}\left(h_i(s)\right)_j\Big|_{s=z_i} & \text{if } \left(h_i(s_i)\right)_j=0\\ 0 & \text{otherwise}\end{cases}$$
$$g_i=\nabla f_i(z_i)$$
$$H_i=\nabla^2\left\{f_i(z_i)+\kappa_i^T h_i(z_i)\right\}$$

5) Solve coupled quadratic program

$$\min_{\Delta z,\xi}\sum_{i\in R}\left\{\begin{aligned}&\frac{1}{2}\begin{pmatrix}\Delta z_{TN} & \Delta z_{DN}\end{pmatrix}\begin{pmatrix}H_{TN} & \\ & H_{DN}\end{pmatrix}\begin{pmatrix}\Delta z_{TN}\\ \Delta z_{DN}\end{pmatrix}\\ &+\begin{pmatrix}g_{TN} & g_{DN}\end{pmatrix}\begin{pmatrix}\Delta z_{TN}\\ \Delta z_{DN}\end{pmatrix}\end{aligned}\right\}+\lambda^T\xi+\frac{\mu}{2}\|\xi\|_2^2$$

$$s.t.\begin{cases}\begin{pmatrix}A_{TN} & A_{DN}\end{pmatrix}\begin{pmatrix}z_{TN}+\Delta z_{TN}\\ z_{DN}+\Delta z_{DN}\end{pmatrix}=\xi\,|\lambda_{\mathrm{QP}}\\ \begin{pmatrix}C_{TN} & \\ & C_{DN}\end{pmatrix}\begin{pmatrix}\Delta z_{TN}\\ \Delta z_{DN}\end{pmatrix}=0\end{cases}$$

6) Update $\begin{pmatrix}s_{TN}\\ s_{DN}\end{pmatrix}\leftarrow\begin{pmatrix}z_{TN}\\ z_{DN}\end{pmatrix}+\begin{pmatrix}\Delta z_{TN}\\ \Delta z_{DN}\end{pmatrix}$, $\lambda\leftarrow\lambda_{\mathrm{QP}}$, $\mu\leftarrow\min\left(\mu,r_\mu\mu\right)$

7) **End while**

IV. CASE STUDIES

A. Basic Settings

In this section, we provide a numerical experiment for the coordinated operation of TN and DN. TN is represented in Fig. 3 by a modified Nguyen-Dupius network, which consists of 13 vertices, 19 arcs, 4 O-D pairs and 7 FCSs. The arcs and O-D data are shown in TABLE I and, respectively. The charging ratio of each O-D pair is γ=1%. The average energy for FCS EV charging on transfer arc is E_{ch}=30kWh, and the charging power is P_{ch}=60kW. Hence, the charging time is t_a^{ch}=30min, where $a\in A_T$. The FCS capacity on a transfer arc is c_a^{ch}=50. The monetary price of travel time is β=10\$/h.

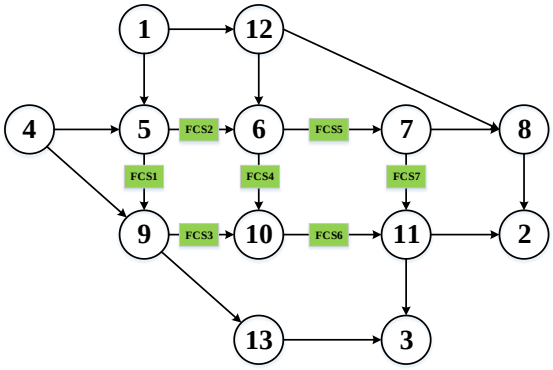

Fig. 3. The topology of Nguyen-Dupius TN

TABLE I
PARAMETERS OF TN ARCS

Entrance	Exit	t_a^0 (min)	c_a (veh)	Entrance	Exit	t_a^0 (min)	c_a (veh)
1	5	7	5000	8	2	9	5000
1	12	9	4000	9	10	10	2000
4	5	9	4000	9	13	9	2000
4	9	12	2000	10	11	6	1000
5	6	3	3000	11	2	9	2000
5	9	9	3000	11	3	8	4000
6	7	5	5000	12	6	7	1000
6	10	13	2000	12	8	14	4000
7	8	5	5000	13	3	11	4000
7	11	9	5000				

TABLE II
TRAFFIC DEMAND OF O-D PAIRS

O-D pairs	1-2	1-3	4-2	4-3
$q_{rs}(1)$ (veh)	1000	1750	1500	750
$q_{rs}(2)$ (veh)	2000	3500	3000	1500
$q_{rs}(3)$ (veh)	2500	4375	3750	1875
$q_{rs}(4)$ (veh)	3000	5250	4500	2250

The modified IEEE 33-bus network represents DN as shown in Fig. 4. The basic data of original IEEE 33-bus network can be found in [37], and the time varying active and reactive loads are shown in Appendix. The DG parameters are given in TABLE III, and the electricity purchase price from the main grid is λ_b=150\$/MWh.

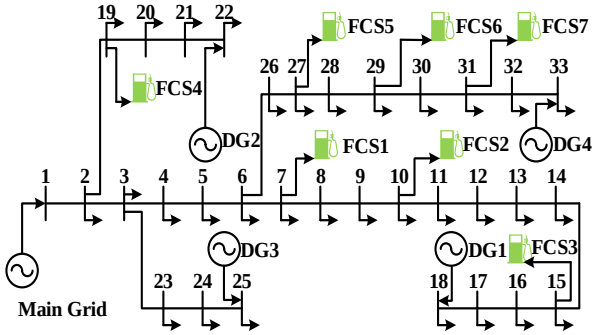

Fig. 4. Topology of IEEE 33-bus network

TABLE III
PARAMETERS OF DGS

Unit	Node	$P_{DG,j}^{\min}$ (MW)	$P_{DG,j}^{\max}$ (MW)	$Q_{DG,j}^{\min}$ ($MVar$)	$Q_{DG,j}^{\max}$ ($MVar$)	a_j ($\frac{\$}{(MW)^2\cdot h}$)	b_j ($\frac{\$}{MW\cdot h}$)
DG1	18	0	4	-2	2	50	100
DG2	22	0	8	-4	4	60	110
DG3	25	0	8	-4	4	70	120
DG4	33	0	6	-3	3	80	130

To discuss the effect of charging price on TN flow assignment and DN reliable operation, we consider a two-stage uncoordinated operation (UCO) mode. At the first stage, the charging prices of all FCSs are set to λ_a^j=0.16\$/*kWh*, and the traffic flow of all arcs is obtained via solving DUE of TN with the constant charging price; then the AC DOPF of DN is solved at the second stage based on traffic flow obtained at the first stage.

B. Proposed Solution Results

The UCO leads to an unsafe DN operation when the traffic flow is very heavy on certain TN arcs. For λ_a^j=0.16\$/*kWh*, the traffic flows on all arcs are calculated according to the DUE of TN. Due to page limitations, we only show in TABLE IV the traffic flow on transfer arcs with FCS during the 4 time periods. Also, the black numbers in Fig. 5. show traffic flows on all arcs at *t*=3 in UCO mode.

Comparing the traffic flows on transfer arcs shown in TABLE IV with the FCS capacities, it is easy to find that FCS2 and FCS5 have always been operated during the 4 time periods, while few EVs are charged in other FCSs. The traffic flows on these transfer arcs are distributed very unevenly. In this case, traffic flows at the transfer arc terminals shown in Fig. 5 do not obey the Kirchhoff's law.

TABLE IV
TRAFFIC FLOW OF TRANSFER ARCS WITH FCSS

		FCS1	FCS2	FCS3	FCS4	FCS5	FCS6	FCS7
t=1	UCO(*veh*)	0	24	1	0	21	2	2
	TDC(*veh*)	0	24	1	0	21	2	2
	λ_a^j(\$)	0.160	0.160	0.160	0.160	0.160	0.160	0.160
t=2	UCO(*veh*)	0	50	0	1	48	1	0
	TDC(*veh*)	17	19	22	18	9	7	9
	λ_a^j(\$)	0.177	0.193	0.175	0.160	0.191	0.161	0.160
t=3	UCO(*veh*)	7	50	6	1	36	3	22
	TDC(*veh*)	22	19	14	7	17	24	22
	λ_a^j(\$)	0.183	0.194	0.186	0.160	0.192	0.160	0.161
t=4	UCO(*veh*)	19	50	11	4	15	22	29
	TDC(*veh*)	25	29	23	12	19	18	24
	λ_a^j(\$)	0.177	0.189	0.176	0.160	0.163	0.162	0.165

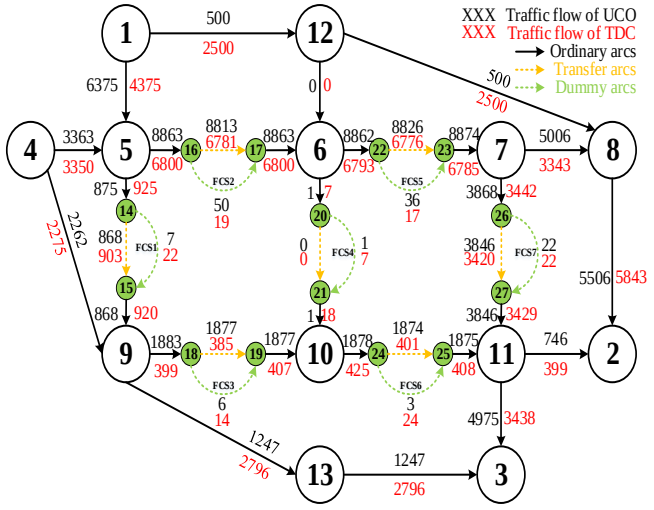

Fig. 5. Traffic flow of all arcs at t=3 in UCO mode and TDC model

Consider the vertex 23 in UCO model, in which the traffic flows of dummy arc and transfer arc between vertices 22 and 23 are 8826 and 36 respectively. However, the traffic flow on the ordinary arc between vertices 23 and 7 is 8874. This seemingly unreasonable condition could be explained by the intertemporal EV charging behaviors between time slots *t* and *t*-1. The assigned 36 EVs is charged in FCS5 at *t*=3; meanwhile the 48 EVs assigned to FCS5 at *t*=2 (see Table IV) have already completed its charging and left the vertex 23. Hence, the traffic flow on the ordinary arc between vertices 23 and 7 is 8826+48=8874. The situations in other vertices and arcs are similar to vertex 23 and FCS5. This observation indicates that the current traffic flow is a function of both traffic flow at present time slot and charged EV at previous time slots, which is consistent with the time coupled traffic flow between *t* and *t*-1 described in (8) and (9).

In UCO mode, the FCS charging load is calculated by (25) using Table IV results. The power flows are calculated by solving the AC DOPF of DN. The voltage magnitude at buses connected with FCS during the 4 time periods are given in TABLE V. We notice that the FCS2 traffic flow is very close to that of FCS5, but the voltage magnitude at bus27 where FCS5 is connected is 0.932 at *t*=2, which is very different from 0.900 at bus10 where FCS2 is connected. The reason is that the nodal voltage magnitude depends not only on EV charging loads but also on the grid topology. Bus27 has a relatively short electrical distance to 33 and its voltage magnitude is higher than that in bus10. To visually demonstrate the results, the bus voltage magnitudes in UCO mode at *t*=3 are shown in Fig. 6, where the bus10 voltage magnitude is approaching its minimum. Because the heavy traffic flow on the transfer arc with FCS2 leads to a large demand at bus10 of DN, the two-stage UCO mode would result in DN bus voltage violations.

TABLE V
VOLTAGE MAGNITUDE OF BUSES CONNECTED TO FCSS

$\|V_j^t\|$ (p.u.)	*t*=1		*t*=2		*t*=3		*t*=4	
	UCO	TDC	UCO	TDC	UCO	TDC	UCO	TDC
7	0.957	0.957	0.939	0.953	0.940	0.950	0.934	0.954
10	0.939	0.939	0.900	0.929	0.900	0.926	0.900	0.932
15	0.957	0.957	0.942	0.944	0.941	0.943	0.936	0.949
19	0.998	0.998	0.998	0.997	0.998	0.997	0.997	0.997
27	0.956	0.956	0.932	0.950	0.937	0.949	0.950	0.953
29	0.964	0.964	0.966	0.963	0.964	0.961	0.956	0.963
31	0.981	0.981	0.986	0.981	0.985	0.981	0.980	0.981

In contrast to UCO, the TN traffic flow and DN power flow are also calculated for the TDC model. The traffic flow of arcs with FCS and charging price of FCS λ_a^j are shown in TABLE IV, and the voltage magnitude of buses connected with FCS are presented in TABLE V. When compare the traffic flow and voltage magnitudes of UCO with that of TDC model at *t*=1, there is not any difference. This is because under light traffic demand $q_{rs}(1)$ at *t*=1, the bus voltage is basically maintained within normal range and the DN operation security has not been threated, therefore the EV charging price is not adjusted and therefore the UCO mode has the same optimal solutions as TDC model. With increasing number of EVs charging in FCSs, the risk of voltage violation will increase rapidly, and FCS charging prices at different locations are adjust to impact the assignation of TN traffic flow and thus results in a reliable for DN power flow distribution to ensure operational security.

In TDC mode, the traffic flow on all arcs in TN at *t*=3 are shown in Fig. 5 and highlighted in red, while the bus voltage magnitudes are shown in Fig. 7. Obviously, the increasing price of FCS2 will lead some EVs to choose other FCSs, which helps alleviate traffic overloads on transfer arc with FCS2. In this way, the voltage magnitude of bus10 is upgraded to its normal level, and the DN security is ensured. Comparing the UCO mode voltage magnitude in Fig. 6 with that of TDC mode

in Fig. 7, it is very clear that the bus voltage is distributed much more evenly in TDC mode.

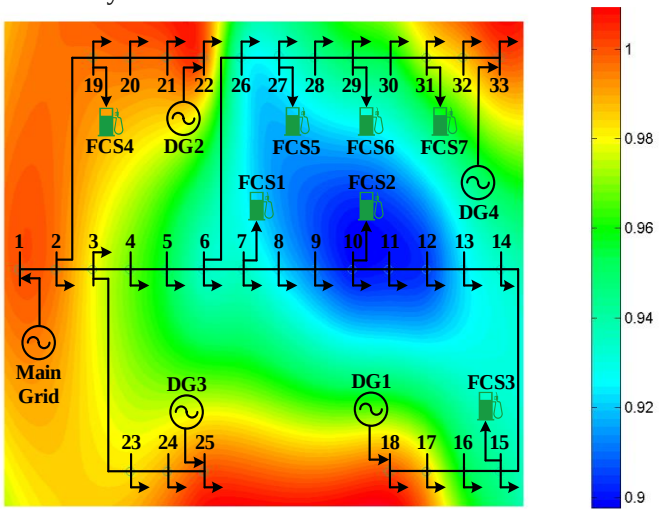

Fig. 6. Voltage magnitude dispersion in UCO mode

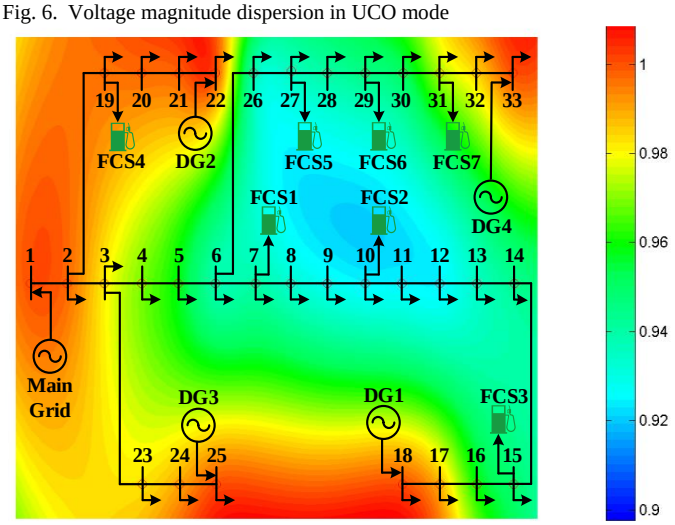

Fig. 7. Voltage magnitude dispersion in TDC mode

C. Proposed Sensitivity analyses

The charging ratio γ influenced by battery capacity, initial state of charge, power consumption per hundred kilometers, and so on will impact the solution of TDC model, and therefore a sensitivity analysis conducted on γ is essential for studying the TDC model. C_{TN} and C_{DN} are correspondingly shown in Fig. 8 by varying γ from 0.5% to 1.5% in 0.25% increments. When $\gamma \leq 0.75\%$, its variation has almost no effect on C_{TN}. This is because the saturation of transfer arc is not deep, and DN constraints are easy to be satisfied without adjusting the charging price. When $\gamma \geq 1\%$, both C_{TN} and C_{DN} continue to grow with an increase in γ. This is because the heavy traffic in FCS will lead to bus voltage violations in DN and the charging price needs to be adjusted to disperse traffic flows in TN. However, if γ is larger than 3 %, the adjustment in charging price will no longer be an effective measure for alleviating DN voltage violations and maintaining TN amenity. The investment on DGs, lines, and FCS, should be considered to alleviate the traffic congestion.

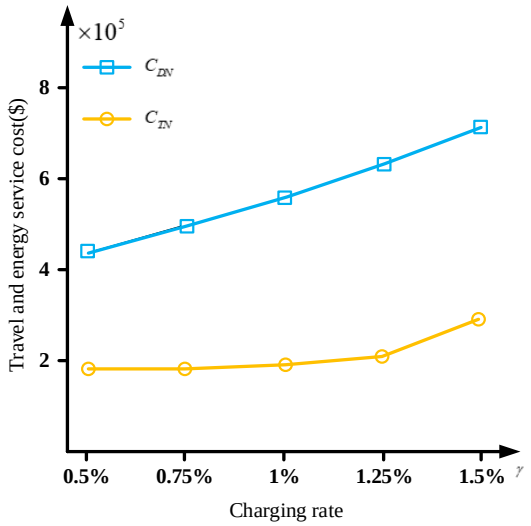

Fig. 8. Sensitivity of charging ratio

V. Conclusion

In this paper, a TDC model which simultaneously considers the DN economic operation and the EV traffic flow assignment in TN, is proposed to minimize the sum of the travel cost of TN and energy service cost of DN. The ALADIN distributed algorithm is presented to effectively solve the TDC model. The case study on an integrated system of the modified Nguyen-Dupius TN and IEEE 33-bus DN has demonstrated the necessity of the coordinated operation of TN and DN. Simulation results have also revealed that the optimal power and traffic flows can be obtained through the solution of the proposed TDC model. In addition, potential DN voltage violations are mitigated by adjusting FCS charging prices in TN.

To replace the average EV charging energy in the TDC model, the heterogeneous EV battery information will be considered in our future work. Besides, we assume the travellers can have access to the full data on traffic arcs and charging prices of FCSs. Accordingly, stochastic user equilibrium will be introduced in TDC to consider the proliferation of variable renewables.

Appendix

TABLE VI
THE ACTIVE AND REACTIVE LOADS OF ALL BUSES

	t=1		t=2		t=3		t=4	
	$P^t_{load,j}$ (kW)	$Q^t_{load,j}$ (kVar)	$P^t_{load,j}$ (kW)	$Q^t_{load,j}$ (kVar)	$P^t_{load,j}$ (kW)	$Q^t_{load,j}$ (kVar)	$P^t_{load,j}$ (kW)	$Q^t_{load,j}$ (kVar)
j=1	0	0	0	0	0	0	0	0
j=2	100	60	200	120	250	150	300	180
j=3	90	40	180	80	225	100	270	120
j=4	120	80	240	160	300	200	360	240
j=5	60	30	120	60	150	75	180	90
j=6	60	20	120	40	150	50	180	60
j=7	200	100	400	200	500	250	600	300
j=8	200	100	400	200	500	250	600	300
j=9	60	20	120	40	150	50	180	60
j=10	60	20	120	40	150	50	180	60
j=11	45	30	90	60	112.5	75	135	90
j=12	60	35	120	70	150	87.5	180	105
j=13	60	35	120	70	150	87.5	180	105

j=14	120	80	240	160	300	200	360	240
j=15	60	10	120	20	150	25	180	30
j=16	60	20	120	40	150	50	180	60
j=17	60	20	120	40	150	50	180	60
j=18	90	40	180	80	225	100	270	120
j=19	90	40	180	80	225	100	270	120
j=20	90	40	180	80	225	100	270	120
j=21	90	40	180	80	225	100	270	120
j=22	90	40	180	80	225	100	270	120
j=23	90	50	180	100	225	125	270	150
j=24	420	200	840	400	1050	500	1260	600
j=25	420	200	840	400	1050	500	1260	600
j=26	60	25	120	50	150	62.5	180	75
j=27	60	25	120	50	150	62.5	180	75
j=28	60	20	120	40	150	50	180	60
j=29	120	70	240	140	300	175	360	210
j=30	200	600	400	1200	500	1500	600	1800
j=31	150	70	300	140	375	175	450	210
j=32	210	100	420	200	525	250	630	300
j=33	60	40	120	80	150	100	180	120

REFERENCES

[1] *Global EV Outlook 2019*, IEA, Paris, France, 2019.

[2] *Innovation outlook: Smart charging for electric vehicles*, IRENA, Abu Dhabi, UAE, 2019.

[3] D. Wu, D. C. Aliprantis, and L. Ying, "Load scheduling and dispatch for aggregators of plug-in electric vehicles," *IEEE Trans. Smart Grid*, vol. 3, no. 1, pp. 368–376, Mar. 2012.

[4] M. E. Khodayar, L. Wu, and M. Shahidehpour, "Hourly coordination of electric vehicle operation and volatile wind power generation in SCUC," *IEEE Trans. Smart Grid*, vol. 3, no. 3, pp. 1271–1279, Sep. 2012.

[5] X. Lu, K. W. Chan, S. Xia, X. Zhang, G. Wang, F. Li, "A Model to Mitigate Forecast Uncertainties in Distribution Systems Using the Temporal Flexibility of Electric Vehicle Aggregators", IEEE Trans. Power Syst., Early Access, 2019. doi: 10.1109/TPWRS.2019.2951108

[6] S. Xia, S. Q. Bu, X. Luo, K. W. Chan and X. Lu, "An Autonomous Real-Time Charging Strategy for Plug-In Electric Vehicles to Regulate Frequency of Distribution System With Fluctuating Wind Generation," *IEEE Transactions on Sustainable Energy*, vol. 9, no. 2, pp. 511-524, April 2018.

[7] R. C. Leou, C. L. Su, and C. N. Lu, "Stochastic analyses of electric vehicle charging impacts on distribution network," I*EEE Trans. Power Syst*., vol. 29, no. 3, pp. 1055–1063, May 2014.

[8] E. Veldman and R. Verzijlbergh, "Distribution grid impacts of smart electric vehicle charging from different perspectives," *IEEE Trans. Smart Grid*, vol. 6, no. 1, pp. 333–342, Jan. 2015.

[9] H. Fan, C. Duan, C. Zhang. "ADMM-Based Multiperiod Optimal Power Flow Considering Plug-In Electric Vehicles Charging," *IEEE Trans. Power Syst.*, vol. 33, no. 4, pp. 3886–3897, Jul 2018.

[10] S. Erdogan and M. H. Elise, "A green vehicle routing problem," *Transp. Res. E*, vol. 48, no. 1, pp. 100–114, 2012.

[11] O. Worley, D. Klabjan, and T. M. Sweda, "Simultaneous vehicle routing and charging station siting for commercial electric vehicles," *Proc. IEEE Int. Elect. Vehicle Conf.*, Greenville, SC, USA, 2012, pp. 1–3.

[12] H. Yang et al., "Electric vehicle route optimization considering time-of-use electricity price by learnable partheno-genetic algorithm," *IEEE Trans. Smart Grid*, vol. 6, no. 2, pp. 657–666, Mar. 2015.

[13] C. Liu, M. Zhou, J. Wu, C. Long and Y. Wang, "Electric Vehicles En-Route Charging Navigation Systems: Joint Charging and Routing Optimization," *IEEE Transactions on Control Systems Technology*, vol. 27, no. 2, pp. 906-914, Mar 2019.

[14] N. Jiang, C. Xie, and S. T. Waller, "Path-constrained traffic assignment: Model and algorithm," *Transp. Res. Rec. J. Transp. Res. Board*, pp. 25–33, Apr. 2012.

[15] T. G. Wang, C. Xie, J. Xie, and T. Waller, "Path-constrained traffic assignment: A trip chain analysis under range anxiety," *Transp. Res. C Emerg. Technol.*, vol. 68, pp. 447–461, Jul. 2016.

[16] G. Wang, Z. Xu, F. Wen and K. P. Wong, "Traffic-Constrained Multiobjective Planning of Electric-Vehicle Charging Stations," *IEEE Transactions on Power Delivery*, vol. 28, no. 4, pp. 2363-2372, Oct. 2013.

[17] S. D. Manshadi, M. E. Khodayar, K. Abdelghany and H. Üster, "Wireless Charging of Electric Vehicles in Electricity and Transportation Networks," *IEEE Transactions on Smart Grid*, vol. 9, no. 5, pp. 4503-4512, Sept. 2018.

[18] F. He, D. Wu, Y. Yin, and Y. Guan, "Optimal deployment of public charging stations for plug-in hybrid electric vehicles," *Transp. Res. B Methodol.*, vol. 47, pp. 87–101, Jan. 2013.

[19] F. He, Y. Yin, J. Wang, and Y. Yang, "Sustainability SI: Optimal prices of electricity at public charging stations for plug-in electric vehicles," *Netw. Spatial Econ.*, vol. 16, no. 1, pp. 131–154, Mar. 2016.

[20] W. Wei, S. Mei, L. Wu, J. Wang and Y. Fang, "Robust Operation of Distribution Networks Coupled With Urban Transportation Infrastructures," *IEEE Transactions on Power Systems*, vol. 32, no. 3, pp. 2118-2130, May 2017.

[21] X. Wang, M. Shahidehpour, C. Jiang and Z. Li, "Resilience Enhancement Strategies for Power Distribution Network Coupled With Urban Transportation System," *IEEE Transactions on Smart Grid*, vol. 10, no. 4, pp. 4068-4079, July 2019.

[22] W. Wei, S. Mei, L. Wu, M. Shahidehpour and Y. Fang, "Optimal Traffic-Power Flow in Urban Electrified Transportation Networks," *IEEE Transactions on Smart Grid*, vol. 8, no. 1, pp. 84-95, Jan. 2017.

[23] M. Alizadeh, H. Wai, M. Chowdhury, A. Goldsmith, A. Scaglione and T. Javidi, "Optimal Pricing to Manage Electric Vehicles in Coupled Power and Transportation Networks," *IEEE Transactions on Control of Network Systems*, vol. 4, no. 4, pp. 863-875, Dec. 2017.

[24] A. Engelmann, Y. Jiang, T. Mühlpfordt, B. Houska, and T. Faulwasser, "Toward Distributed OPF using ALADIN," *IEEE Trans. Power Syst.*, vol. 34, no. 1, pp. 584–594, Jan. 2019.

[25] S. Peeta and A. K. Ziliaskopoulos, "Foundations of dynamic traffic assignment: The past, the present and the future," *Netw. Spat. Econ.*, vol. 1, no. 3, pp. 233–265, Sep. 2001.

[26] Y. Sheffi, *Urban Transportation Networks*. Englewood Cliffs New Jersey: Prentice-Hall, 1985.

[27] W. Wei, L. Wu, J. Wang and S. Mei, "Network Equilibrium of Coupled Transportation and Power Distribution Systems," *IEEE Transactions on Smart Grid*, vol. 9, no. 6, pp. 6764-6779, Nov. 2018.

[28] Q. Guo, S. Xin, H. Sun, Z. Li, and B. Zhang, "Rapid-charging navigation of electric vehicles based on real-time power systems and traffic data," *IEEE Trans. Smart Grid*, vol. 5, no. 4, pp. 1969–1979, Jul. 2014.

[29] Bureau of Public Roads, "Traffic assignment manual," U.S. Dept. Commerce, Washington, DC, USA, 1964.

[30] K. B. Davidson, "A flow-travel time relationship for use in transportation planning," in *Proc. Aust. Road Res. Board*, Melbourne, VIC, Australia, 1966, pp. 183–194.

[31] P. Kachroo, N. Shlayan. *Dynamic Traffic Assignment: A Survey of Mathematical Models and Techniques*, New York: Springer, 2013.

[32] Q. Peng and S. H. Low, "Distributed Optimal Power Flow Algorithm for Radial Networks, I: Balanced Single Phase Case," *IEEE Transactions on Smart Grid*, vol. 9, no. 1, pp. 111-121, Jan. 2018.

[33] S. Mhanna, G. Verbič and A. C. Chapman, "Adaptive ADMM for Distributed AC Optimal Power Flow," *IEEE Transactions on Power Systems*, vol. 34, no. 3, pp. 2025-2035, May 2019.

[34] M. Farivar and S. H. Low, "Branch flow model: Relaxations and convexification (parts I, II)," *IEEE Trans. Power Syst.*, vol. 28, no. 3, pp. 2554–2572, 2013.

[35] L. Gan, N. Li, U. Topcu and S. H. Low, "Exact Convex Relaxation of Optimal Power Flow in Radial Networks," *IEEE Transactions on Automatic Control*, vol. 60, no. 1, pp. 72-87, Jan. 2015.

[36] B. Houska, J. Frasch, and M. Diehl, "An augmented lagrangian based algorithm for distributed nonconvex optimization," *SIAM J. Optim.*, vol. 26, no. 2, pp. 1101–1127, 2016.

[37] M. Baran and F. Wu, "Network reconfiguration in distribution systems for loss reduction and load balancing," *IEEE Trans. on Power Delivery*, vol. 4, no. 2, pp. 1401–1407, Apr. 1989.

Guangzeng Sun (S'16) received the B.Sc. degree in electrical engineering from North China Electric Power University, Beijing, China, in 2016. He is currently working toward the Ph.D. degree in electrical engineering with North China Electric Power University, Beijing, China. His areas of interest include coordinated operation of traffic network and distribution network.

Gengyin Li (M'03) received the Ph.D. degree in electrical engineering from North China Electricity Power University, Beijing, China, in 1996. He is currently a professor in the School of Electrical and Electronic Engineering, North China Electricity Power University. His research interests include HVDC transmission, power quality analysis and control, and new transmission and distribution technologies.

Shiwei Xia (SM'20) received the Ph.D. degree in power systems from The Hong Kong Polytechnic University, Hung Hom, Hong Kong, in 2015. Currently, he is with the State Key Laboratory of Alternate Electrical Power System with Renewable Energy Sources, School of Electrical and Electronic Engineering, North China Electric Power University, Beijing, China, and also a Visiting Faculty with the Robert W. Galvin Center for Electricity Innovation, Illinois Institute of Technology, Chicago, IL, USA. His research interests include security and risk analysis for power systems with renewables, distributed optimization and control of AC-DC distribution grid.

Mohammad Shahidehpour (F'01) received the Honorary Doctorate degree in electrical engineering from the Polytechnic University of Bucharest, Bucharest, Romania. He is the Bodine Chair Professor and the Director with the Robert W. Galvin Center for Electricity Innovation, Illinois Institute of Technology, Chicago, IL, USA. He is a member of the US National Academy of Engineering, Fellow of IEEE, Fellow of the American Association for the Advancement of Science (AAAS), and Fellow of the National Academy of Inventors (NAI).

Xi Lu received the B.Sc. degree in electrical engineering from the North China Electric Power University, Beijing, China, in 2015. He is currently working toward the Ph.D. degree in electrical engineering with the Hong Kong Polytechnic University, Hong Kong. His research interests include the application of robust optimization and distributionally robust optimization in power system operation.

Ka Wing Chan (M'98) received the B.Sc. (with First Class Honors) and Ph.D. degrees in electronic and electrical engineering from the University of Bath, Bath, U.K., in 1988 and 1992, respectively. He currently is an Associate Head and Associate Professor in the Department of Electrical Engineering of The Hong Kong Polytechnic University. His general research interests include smart grid and renewable energy, power system stability analysis and control, power system planning and optimization, real-time power system simulation.